Electronic Supplementary Material (ESI) for ChemComm.
This journal is © The Royal Society of Chemistry 2024

Plastron effect enhanced electrochemical CO_2 reduction activity over hydrophobic three-dimensional nanoporous silver

Experimental section

Materials. Silver nitrate($AgNO_3$, 99.9%), Polyvinylpyrrolidone(PVP_{k30}, 99%), Potassium bicarbonate ($KHCO_3$, 99.5%), Nafion (5 wt%, 99%), Carbon paper (SGL-28BC), Sodium oxalate($Na_2C_2O_4$, 99.8%). Potassium hydroxide(KOH, 99.0%), Silver nanoparticles(99.9%), Silver foil (99.999%). All reagents were of analytical grade and used without further purification.

Characterization. X-ray diffraction (XRD) patterns of the catalysts were collected on a DX2700 diffractometer with Cu Kα radiation (λ = 1.5406 Å). Under 10kV voltage, the morphology and structure of the catalyst were characterized by S8230 scanning electron microscope (SEM, Hitachi, Japan). The static contact angles of the catalysts were carried out using a SUNZERN contact angle meter (SZ-CAMC11). CO_2 adsorption and desorption test was performed using a QuadraSorb Station 1 specific surface area tester from Conta Instruments, USA, with a degassing temperature of 273 K and a degassing time of 8 hours.

Synthesis of $Ag_2C_2O_4$. First, 0.510 g $AgNO_3$ was dissolved in 30 ml ultrapure water, stirred, and transferred to a 100 ml three-necked flask. The flask was equipped with a 600 $r \cdot min^{-1}$ magnetic stirrer, and the solution was condensed and refluxed at 60 ℃. Next, a certain amount of PVP_{k30} was dissolved in 10 ml of ultrapure water, stirred, and then added dropwise at a constant rate to the above $AgNO_3$ solution and then reacted at 60 ℃ for 1 h. Eventually, 0.201 g $Na_2C_2O_4$ was dissolved in 40 ml of ultrapure water, stirred, and then added dropwise at a constant rate to the above solution and then reacted at 60 ℃ for 3 h. The product was collected by centrifugation (10 min, 4000 rpm), washed with ultrapure water twice, then with ethanol once, and dried under a vacuum oven.

Synthesis of AgHN. To prepare the ink solution, 0.2 mmol of $Ag_2C_2O_4$ were dissolved in 950 μL of ethanol. Subsequently, 50 μL of 5 wt % Nafion was added as a

binder, followed by ultrasonication for 30 min to ensure homogeneous dispersion. Approximately 100 μL of the ink was uniformly spread over a 1 cm × 1 cm section of the treated carbon paper and dried at 60 ℃ for 10 min. The Ag electrocatalyst was obtained by simple electrochemical reduction of $Ag_2C_2O_4$ by chronoamperometry at a potential of -0.4 V (vs RHE) for 300 s in N_2-saturated 0.5 M $KHCO_3$.

Synthesis of AgHN-VA, AgHN-ETOH, AgHN-VA-ETOH, and AgHN-ETOH-Dry. All four catalysts were obtained from AgHN by different treatments in a standard H-cell system.

(a)AgHN-VA. After the reduction of $Ag_2C_2O_4$ to AgHN, the air in the cathode chamber was extracted to expel the gas from the porous structure, the electrode was labeled as AgHN-VA.

(b)AgHN-ETOH. After reducing $Ag_2C_2O_4$ to AgHN, the electrolyte in the cathode chamber was replaced with ethanol and immersed for some time, and then the ethanol was replaced with electrolyte, and the electrode was noted as AgHN-ETOH.

(c) AgHN-VA-ETOH. After $Ag_2C_2O_4$ was reduced to AgHN, the electrolyte in the cathode chamber was replaced with ethanol, and then the air in the cathode chamber was extracted. After the extraction was completed, the ethanol was replaced with the electrolyte and extracted again, and the electrode was recorded as AgHN-VA-ETOH.

(d) AgHN-ETOH-Dry. AgHN-VA-ETOH was dried to remove the electrolyte present in the nanopores to obtain AgHN-ETOH-Dry.

Electrochemical testing. All of the electrochemical experiments were performed using a standard three-electrode configuration. A saturated KCl solution with Ag/AgCl acted as the reference electrode, and a Pt mesh functioned as the counter electrode. Both working and reference electrodes were positioned in the cathode chamber, with the Pt mesh in the anode chamber. Both chambers were filled with 40 mL of 0.5 M $KHCO_3$ and separated by a Nafion 117 membrane. First, the cathode chamber was purged with N_2 at 40 mL·min^{-1} for 30 min to remove residual oxygen. Subsequently, a potential of -0.4 V(vs RHE) was applied to reduce the precursor to obtain the silver electrocatalysts. Eventually, CO_2 was passed into the electrolyte of the cathode chamber until saturation, followed by the reduction reaction of CO_2. All potentials presented were referenced to the reversible standard hydrogen potential (RHE), with corrections implemented by iR, E(vs RHE, iR) = E(vs Ag/AgCl) + 0.197 + 0.0592×pH-iRu.

Product Analysis. Gas chromatography (GC 2014 C) was used for periodic analyses at 12-minute intervals at each established potential. This enabled the quantification of CO and H_2 concentrations in the cathode chamber via a hydrogen flame ionization detector (FID1) for CO and CH_4 and a thermal conductivity detector (TCD) for H_2.

The Faraday efficiencies for CO and H_2 were deduced from the formula:

$$FE(\%) = \frac{n \times z \times \mathrm{F}}{I \times t} \times 100\% = \frac{2 \times V \times 10^{-9} \times 96485}{22.4 \times I \times \frac{60}{u}}$$

Within the equation, FE signifies the Faraday efficiency specific to a product; n is the moles (mol) of the CO product; z (equal to 2 in this context) signifies electrons transferred during CO_2 reduction to CO; F is the Faraday constant (96485 C·mol^{-1}); I represents the current (A); t stands for the time (in s) required to flow 1 mL of gas; V denotes the quantity of a specific product per 1 mL of feed gas (in ppm); and u indicates the CO_2 gas flow rate (20 mL·min^{-1} in this work).

Electrochemical active surface area (ECSA) Measurement. The monolayer oxidation method was used to determine the ECSA of the catalysts. The cyclic voltammetry curve of Ag foil was first tested in N_2-saturated 0.1 M KOH solution, as shown in Fig. S20, which shows three oxidation peaks. It is generally believed that the first peak located at 1.15 V (vs RHE) is the monoatomic layer oxidation peak of silver. This potential is the monoatomic layer oxidation potential of silver. These three Ag catalysts were oxidized at 1.15 V (vs RHE), which was believed to only form a monolayer of Ag_2O or AgOH, corresponding to a charge of about 400 μC cm^{-2}. By comparing the amount of electrons passed during the oxidation process, the relative surface areas between different Ag catalysts can be obtained. Therefore, the specific ECSA of silver-based catalysts can be calculated as follows[1–3]:

$$\mathrm{ECSA} = Q_\mathrm{r} / (Q_0 * A)$$

where Q_r is the total amount of charge consumed during the electrochemical oxidation process on different silver-based catalysts, Q_0 is the amount of charge consumed to produce an atomic Ag_2O or AgOH monolayer (Q_0 = 400 μC cm^{-2}) on a smooth silver surface,[1–4] A is geometric area of the electrodes (cm^2).

Electrochemical Impedance Spectroscopy(EIS) Measurement. EIS measurement was performed in CO_2-saturated 0.5 M $KHCO_3$ at an open circuit

potential (OCP) of 0.1 Hz ~ 100 kHz, with an amplitude value of 5 mV of the applied voltage. Data was fitted by the Nova software (version 2.1).

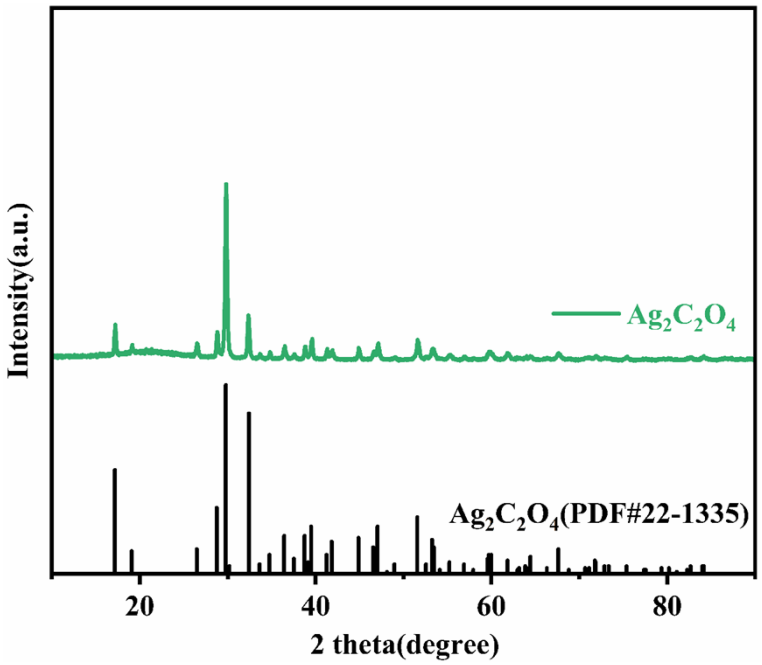

Fig. S1 XRD pattern of $Ag_2C_2O_4$.

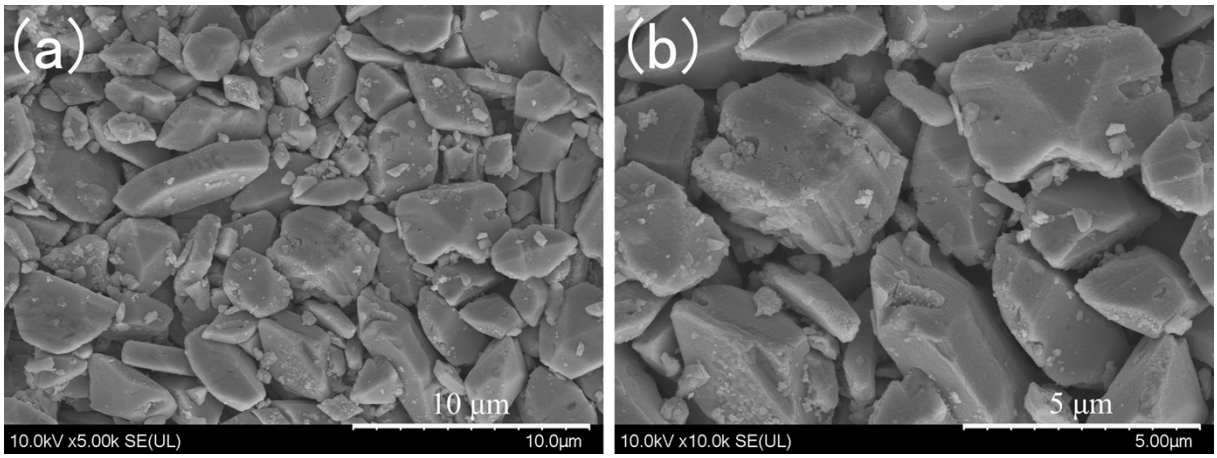

Fig. S2 Low and high magnification SEM images of $Ag_2C_2O_4$.

A cyclic voltammetry test was performed in 0.5 M $KHCO_3$ saturated with N_2 to determine the reduction potential for $Ag_2C_2O_4$ (Fig. S3a). A reduction peak is observed at the potential of about 0.58 V(vs RHE), representing the lowest applied potential for reducing $Ag_2C_2O_4$ to Ag. The magnitude of the reduction potential falls within the range of 0.70 V - 0.50 V, which implies that $Ag_2C_2O_4$ can be reduced to Ag with reduction potentials lower than 0.50 V (vs RHE). To obtain a quick reduction, we chose -0.4 V(vs RHE) as the reduction potential.

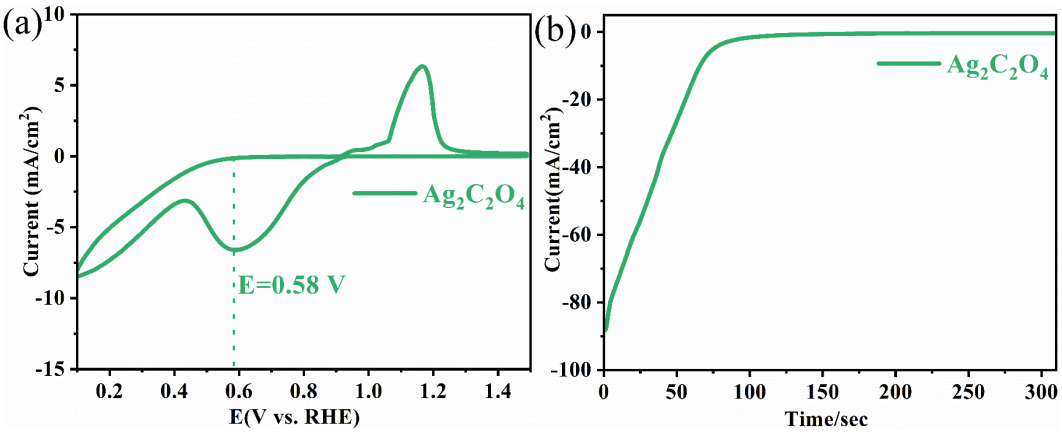

Fig. S3 (a) Cyclic voltammetry curve of $Ag_2C_2O_4$ in 0.5 M $KHCO_3$ saturated with N_2. (b) i-t diagram of the reduction of $Ag_2C_2O_4$ to AgHN.

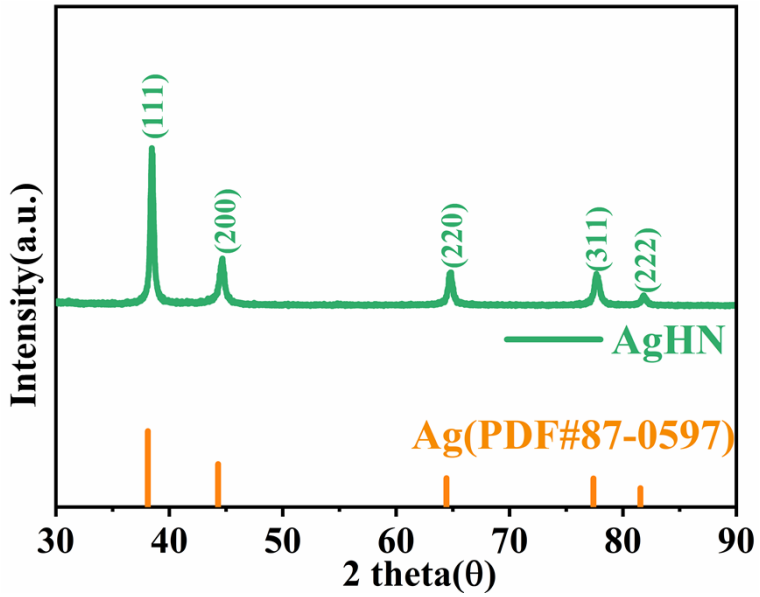

Fig. S4 XRD pattern of AgHN.

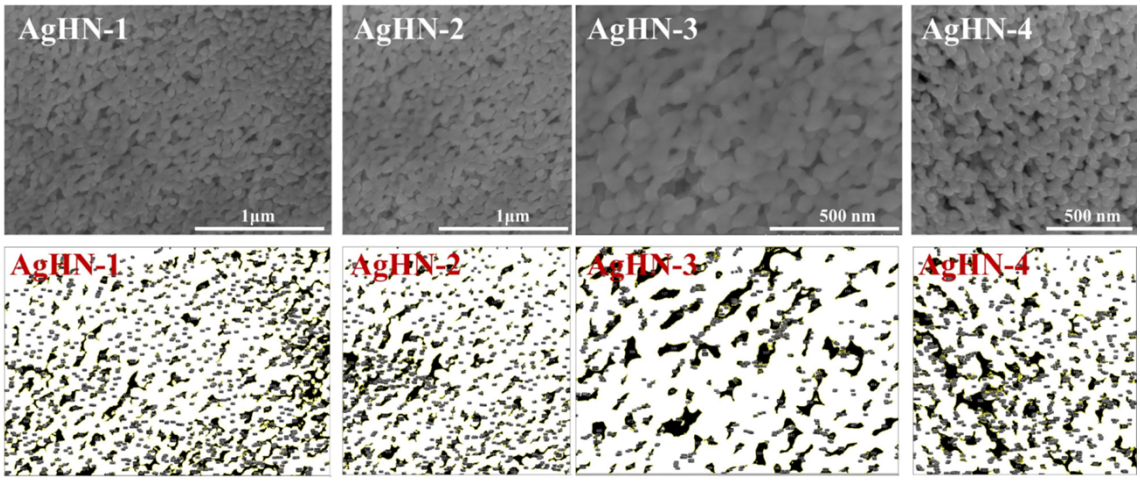

Fig. S5 Pore distribution map of AgHN.

Table S1 The porosity of AgHN.

Catalyst	Number of pores	Hole area	Total area	Porosity (%)
AgHN-1	759	117201	802816	14.599
AgHN-2	622	179789	1149440	15.641
AgHN-3	1039	69375	404471	17.152
AgHN-4	1029	190220	1146880	16.586

AgHN-X(X=1,2,3,and 4) represents different regions of the same AgHN.

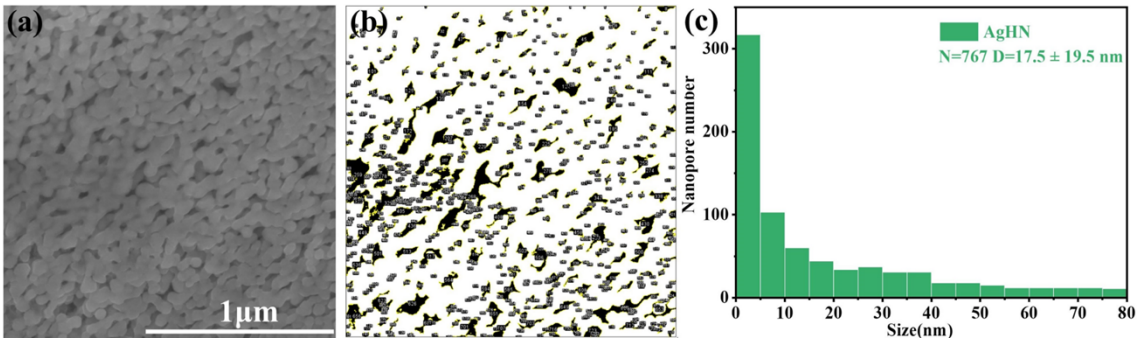

Fig. S6 Pore size distribution map of AgHN.

XRD and SEM images of Ag foil and AgNPs are shown in Fig. S7 and Fig. S8. The static contact angles of Ag foil, AgNPs, and AgHN are shown in Fig. S9, and it can be seen that Ag foil is hydrophilic in both CO_2-saturared 0.5 M $KHCO_3$ and water, while both AgNPs and AgHN are hydrophobic.

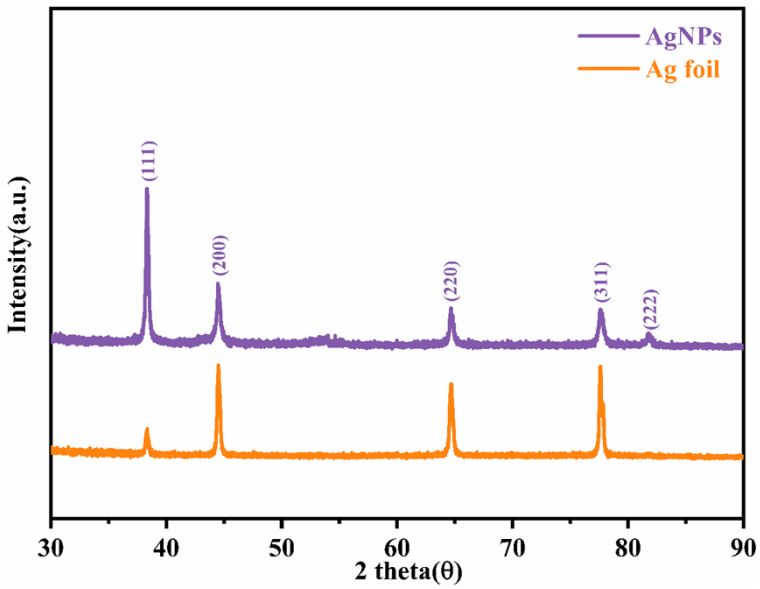

Fig. S7 XRD patterns of AgNPs and Ag foil.

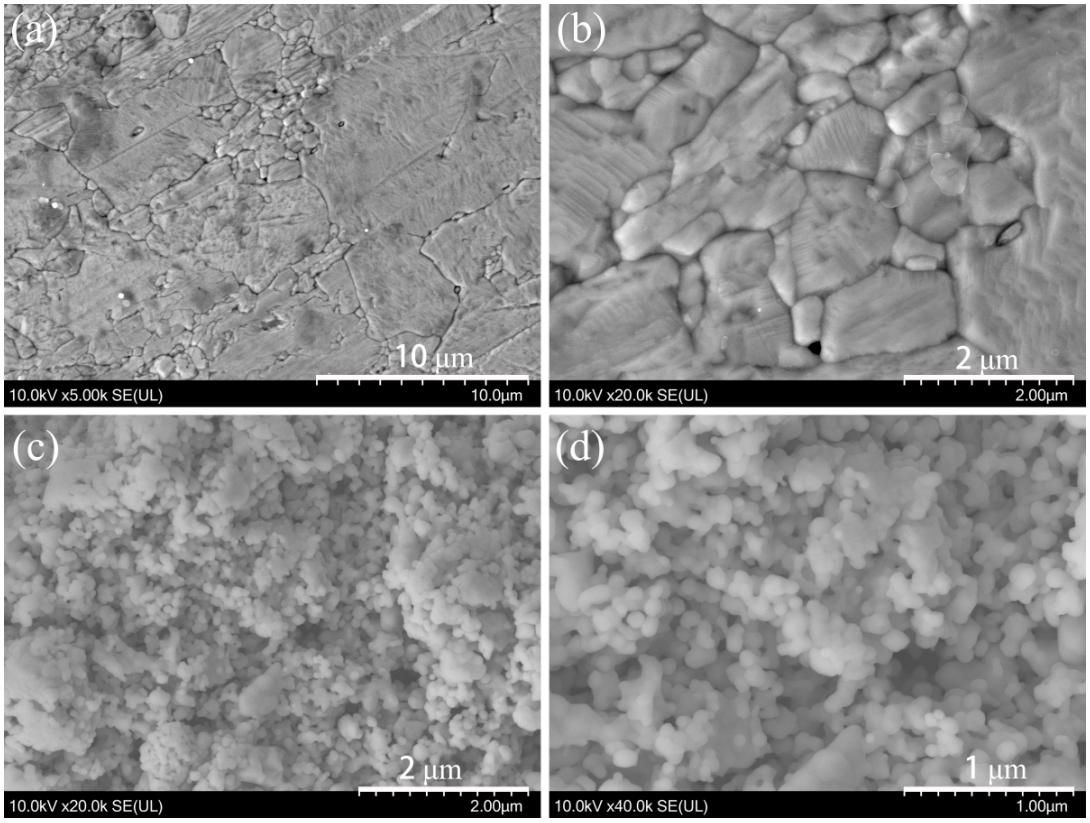

Fig. S8 SEM images of Ag foil(a,b) and AgNPs(c,d).

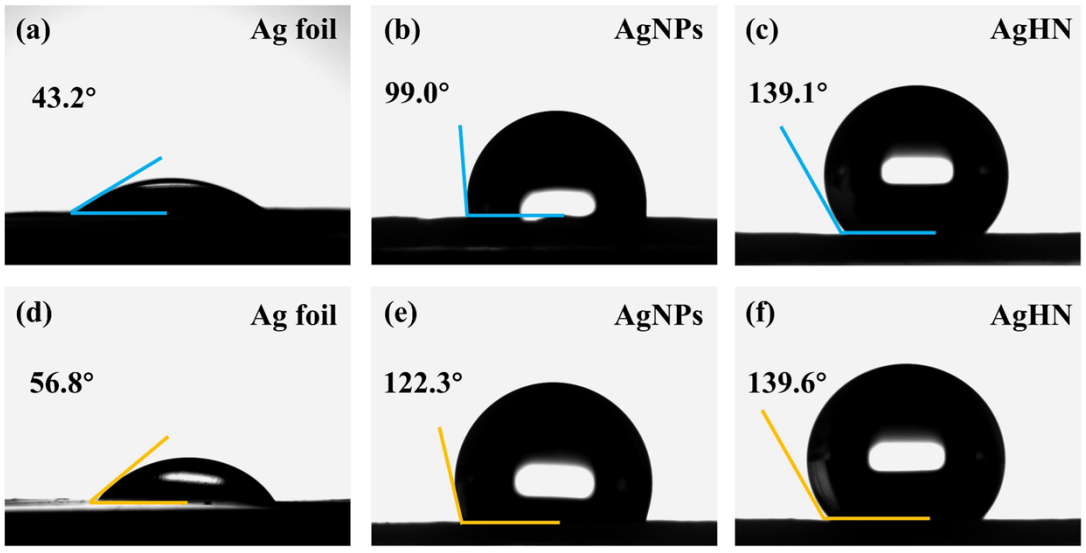

Fig. S9 Static contact angles of Ag foil(a), AgNPs(b), and AgHN(c) in water. Static contact angles of Ag foil(d), AgNPs(e), and AgHN(f) using CO_2-saturared 0.5 M $KHCO_3$ as the liquid.

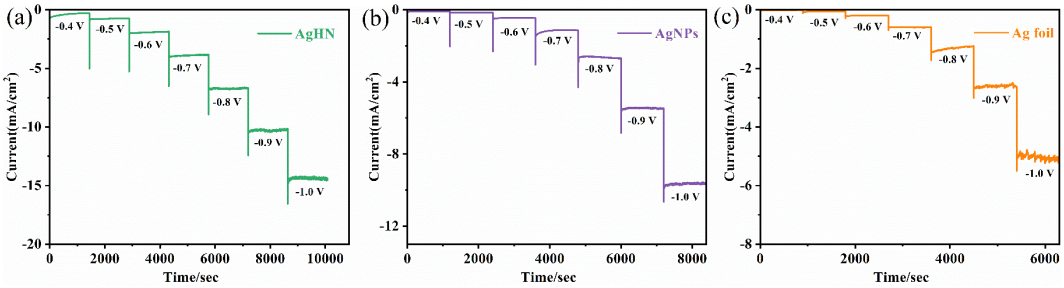

Fig. S10 The i-t curves of AgHN(a), AgNPs(b), and Ag foil(c).

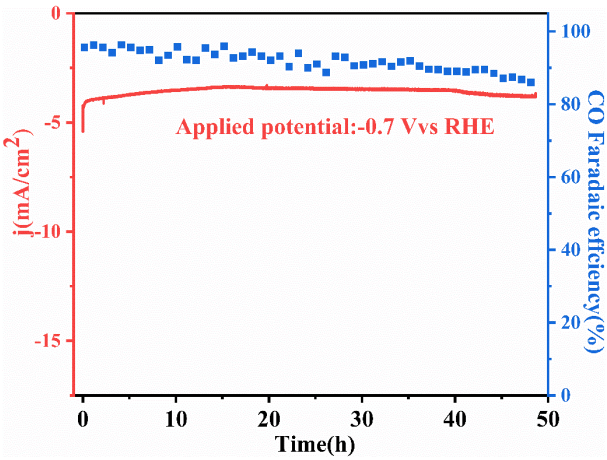

Fig. S11 Recorded chronoamperometric curve from AgHN at −0.7 V versus RHE over a 48 h period and the corresponding FE_{CO}.

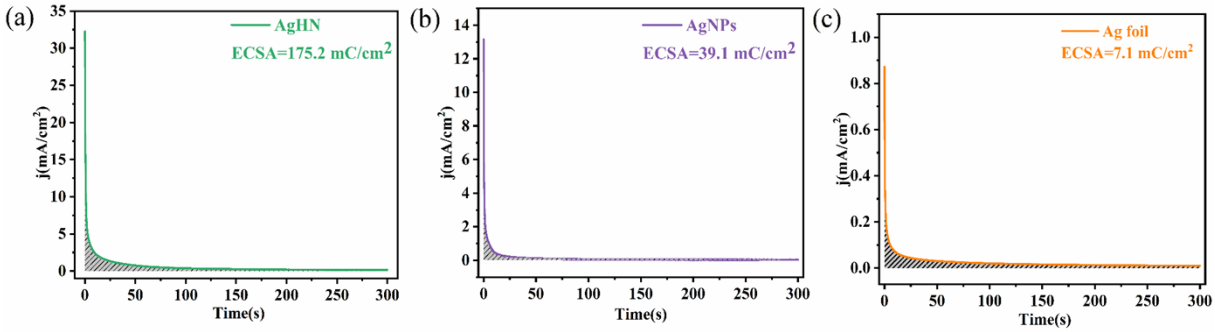

Fig. S12 ECSA of AgHN(a), AgNPs(b), and Ag foil(c).

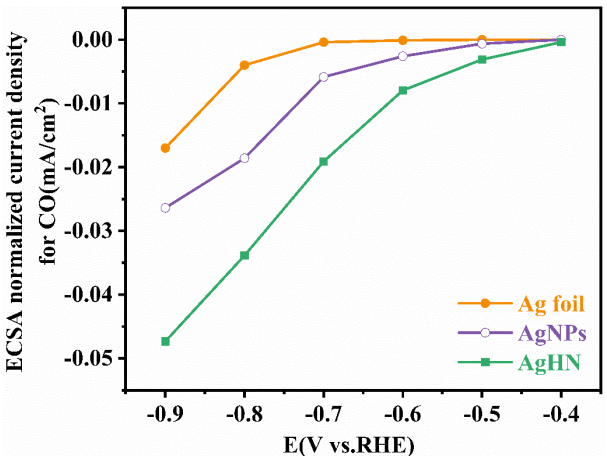

Fig. S13 Potential dependence of ECSA normalized current density for CO on the AgHN, AgNPs, and Ag foil.

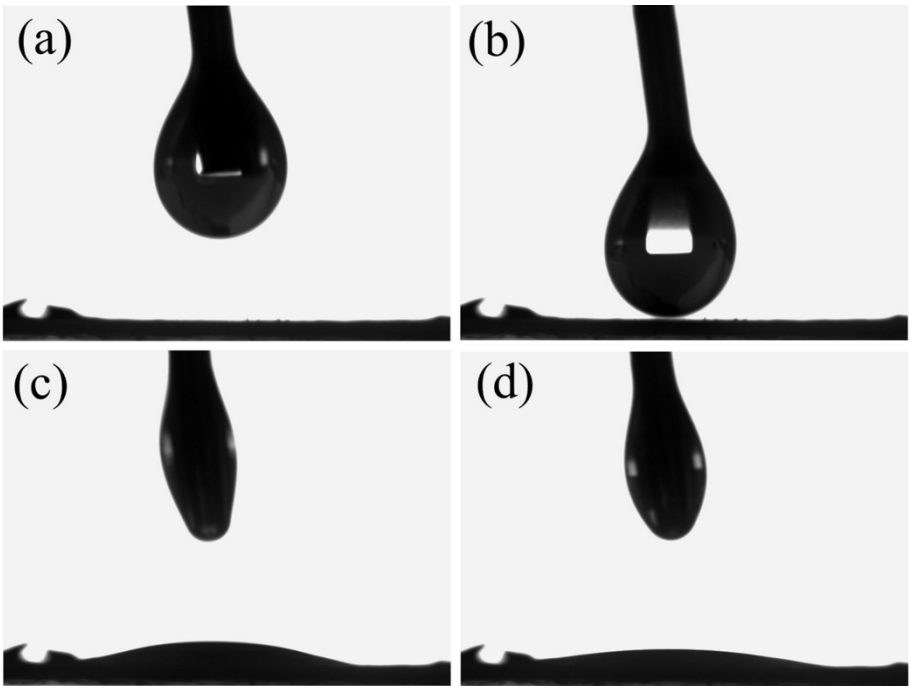

Fig. S14 Static contact angle of AgHN under ethanol.

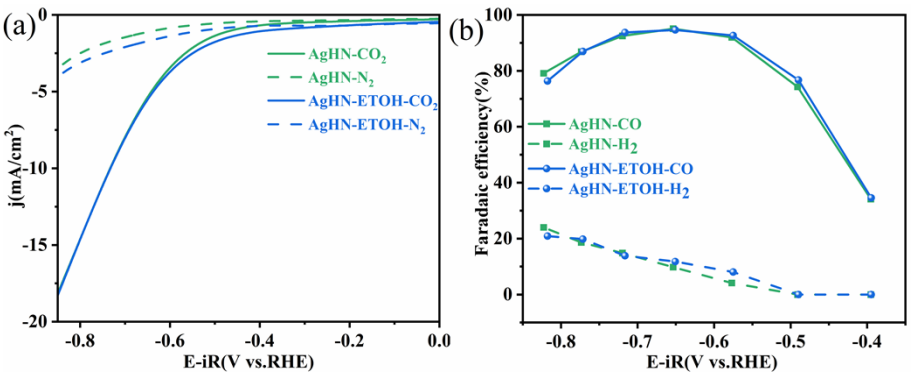

Fig. S15 Comparison of catalytic performance of AgHN-ETOH and AgHN, (a)LSV, (b)FE.

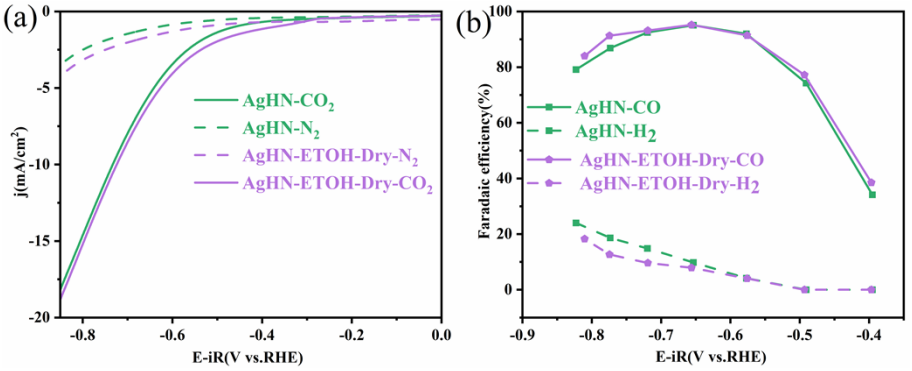

Fig. S16 Comparison of catalytic performance of AgHN-ETOH-Dry and AgHN,

(a)LSV, (b)FE.

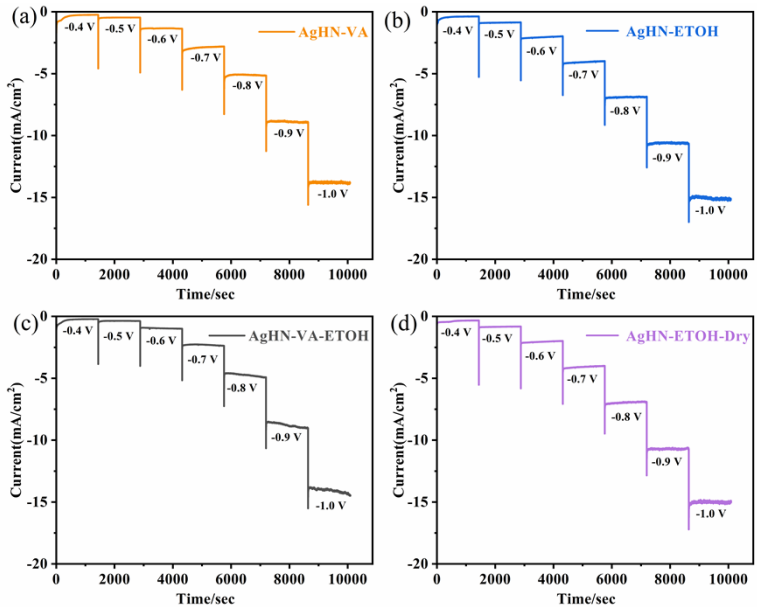

Fig. S17 The i-t curves of AgHN-VA(a), AgHN-ETOH(b), AgHN-VA-ETOH(c), and AgHN-ETOH-Dry(d).

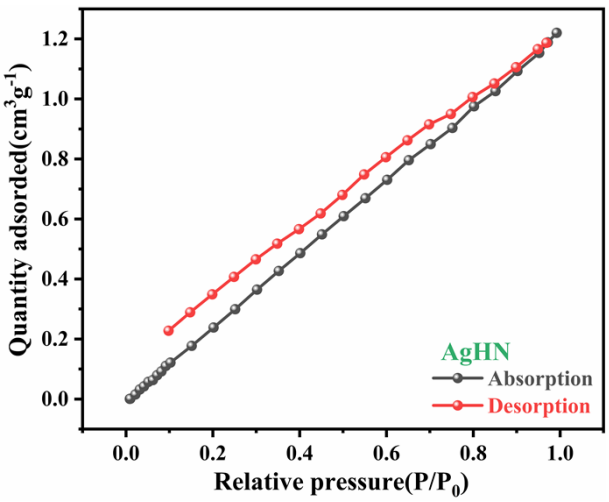

Fig. S18 CO_2 adsorption-desorption isotherms curve of AgHN at 273 K.

The static contact angles of AgHN, Ag-VA-ETOH, AgHN-VA, and AgHN-ETOH-Dry are shown in Fig. S19. When the nanopores of AgHN are filled with ethanol or electrolyte, the static contact angle decreases. The static contact angle of AgHN-VA is 100.1°, while that of AgHN-VA-ETOH is 43.5°. When AgHN-VA-ETOH was dried to obtain AgHN-ETOH-Dry, its static contact angle increased(140.4°) and approached that of AgHN(139.6°).

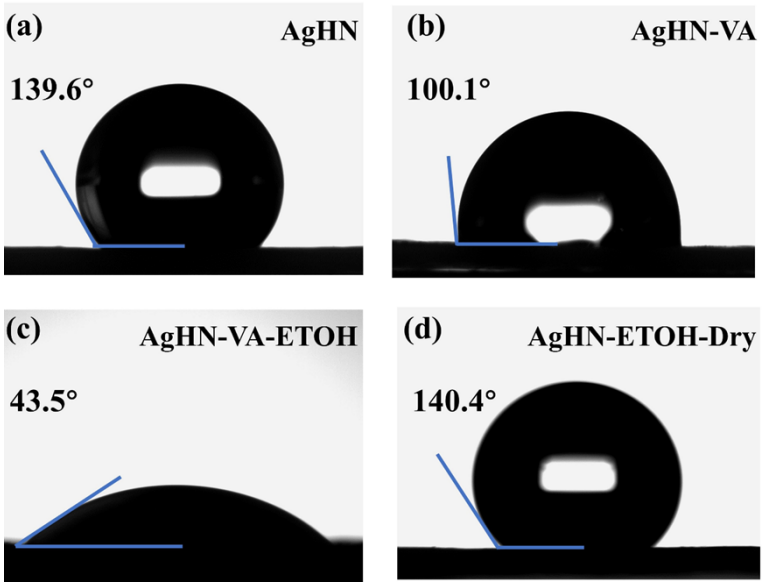

Fig. S19 Static contact angles of AgHN(a), AgHN-VA(b), AgHN-VA-ETOH(c), and AgHN-ETOH-Dry(d) using CO_2-saturared 0.5 M $KHCO_3$ as the liquid.

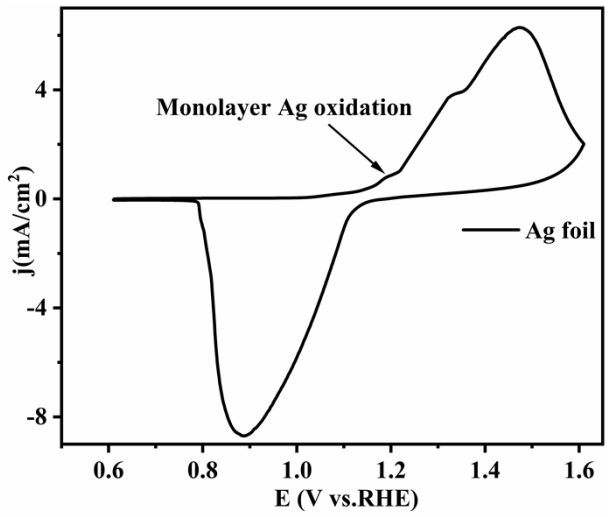

Fig. S20 Cyclic voltammetry of Ag foil in N_2-saturated 0.1 M KOH.

1 K. Ye, T. Liu, Y. Song, Q. Wang and G. Wang, *Applied Catalysis B: Environmental*, 2021, **296**, 120342.

2 L. Wei, H. Li, J. Chen, Z. Yuan, Q. Huang, X. Liao, G. Henkelman and Y. Chen, *ACS Catal.*, 2020, **10**, 1444–1453.

3 Q. Lu, J. Rosen, Y. Zhou, G. S. Hutchings, Y. C. Kimmel, J. G. Chen and F. Jiao, *Nat Commun*, 2014, **5**, 3242.

4 J. Gomez Becerra, R. C. Salvarezza and A. J. Arvia, *Electrochimica Acta*, 1988, **33**, 1431–1437.